Acta Chemica Scandinavica, 1994: 48: 445–452
Printed in Belgium – all rights reserved

ACTA
CHEMICA SCANDINAVICA
ISSN 0904–213X

Carbonate Esters and Double Esters. Optimisation using Statistical Design and Analysis. Monitoring by Fiber-Optical NIR Spectroscopy

Hans-René Bjørsvik

NYCOMED Imaging AS, Department of Process Chemistry, P.O. Box 4220 Torshov, N-0401 Oslo, Norway

Bjørsvik, H.-R., 1994. Carbonate Esters and Double Esters. Optimisation using Statistical Design and Analysis. Monitoring by Fiber-Optical NIR Spectroscopy. – Acta Chem. Scand. 48: 445–452 © Acta Chemica Scandinavica 1994.

Statistical experiment design and analysis have been applied to a study of the synthetic transformation of an acid into a double ester. The objectives were to explore the influence of those independent variables and their interactions which were expected to influence the synthetic reaction. The model obtained was used to predict optimal conditions, in order to establish a high-yielding synthetic procedure for making 1-(ethoxycarbonyloxy)ethyl 5-acetamido-3-(*N*-methylacetamido)-2,4,6-triiodobenzoate, a substance of interest as an X-ray contrast agent for the medical imaging of the liver.

A new technique based upon fiber-optical near infrared spectroscopy and principal components analysis has been developed and applied to monitor the concentration profile over time for the synthetic reaction and to determine the optimal reaction time.

In the field of antibiotics, application of the prodrug concept has, for example, led to improvement in the poor absorption of ampicillin from the gastrointestinal tract.[1] By the use of double esters or carbonate esters in ampicillin, to obtain, e.g., bacampicillin [ampicillin–$CH(CH_3)$ $O(CO)OCH_2CH_3$] or pivampicillin [ampicillin–$CH_2O(CO)OC(CH_3)_3$], the absorption of the modified ampicillin, the prodrug, is highly increased. The absorbed prodrug is rapidly hydrolyzed *in vivo*, to the active compound by non-specific esterases.

Thus, these biodegradable double esters and carbonate esters are attractive owing to the good absorption properties as well as the very large difference between *in vitro* and *in vivo* stability.

In our laboratory, the prodrug concept was introduced in the design of X-ray contrast agents[2] for computer-tomographic (CT) study of the liver.[3–5] By introduction of the $-CH(CH_3)$ $O(CO)OCH_2CH_3$ moiety (as in bacampicillin) into 5-acetamido-3-(*N*-methylacetamido)-2,4,6-triiodobenzoic acid, **1** (metrizoic acid), the product 1-(ethoxycarbonyloxy)ethyl 5-acetamido-3-(*N*-methylacetamido)-2,4,6-triiodobenzoate, **3** (Scheme 1) becomes water insoluble. Thus, after intravenous administration of the particulate aqueous suspension of the X-ray contrast agent, the particulate material is taken up by the Kupffer cells of the liver. The liver macrophage enzymes hydrolyze the carbonate ester of metrizoic acid **3** which then gives a homogenous distribution of the X-ray contrast moiety in the liver.[5]

Thus, the introduction of a double ester or carbonate ester moiety into many types of acid has become an important synthetic step in various synthetic procedures in the pharmaceutical industry.

The present paper describes a statistically designed screening study with the purpose of determining which experimental variables are important as well as making a

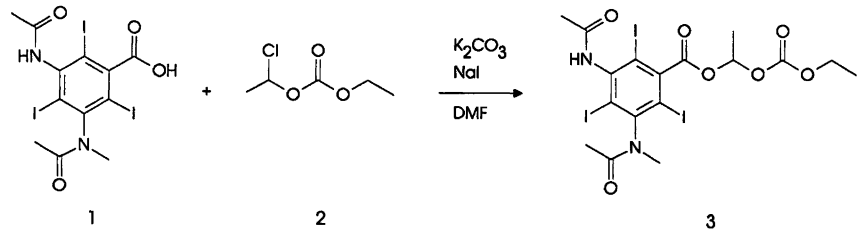

1 2 3

Scheme 1.

survey of the optimal conditions for the double ester formation reaction, with special regard to the synthetic procedure for **3**.

Scheme 2.

Methods and results

Experimental variables and domain. The statistical experimental design was adressed to answer the following questions. (*i*) Are the conditions for the organic synthesis in the proper domain? (*ii*) Which variables influence the outcome of the synthesis, and what is the relationship between them? (*iii*) Is there also influence from interaction terms of the experimental variables in the explored region? (*iv*) What are the best settings of the variables to obtain a high yielding procedure?

The explored domain is specified in Table 1 and a brief discussion of the experimental variables and their settings follows.

Amount of potassium carbonate x_1. The basicity of the reaction mixture may influence the yields of degradation products. Thus, it is important to spot the role of potassium carbonate in the synthesis. In addition, a good procedure from an economical point of view would be to use only the amount of potassium carbonate required to make the substrate, **1**, soluble in the solvent *N,N*-dimethylformamide (DMF).

Sodium iodide as catalyst x_2. It has been suggested that addition of sodium iodide is beneficial for the halodehalogenation reaction, also known as the Finkelstein reaction.[6] An explanation for this is that replacement of a light halogen by a heavier one in an agent often gives an improved result because of the introduction of a better leaving group (see Ref. 7). The sodium iodide catalyzed reaction has also been applied in a similar reaction: introduction of lipophilic moieties in penicillins.[8] Thus, addition of sodium iodide to the reaction mixture might be expected to yield an intermediate iodine-substituted reagent in the present reaction, Scheme 2, which might increase the rate and hence the overall yield over time.

Concentration of **1** *in DMF* x_3. In a large scale synthesis, it is advantageous if the reaction can be carried out at as high a concentration as possible. There are several reasons: (*i*) cost, (*ii*) increased production capacity, and (*iii*) improved environmental aspects, with respect both to the working atmosphere and to the waste problems. Thus, the preferred conditions should be to run the synthesis at high substrate concentration.

Amount of **2** x_4. From an economical point of view, stoichiometric amounts of substrate and reagents should be used. If an acceptable yield could be obtained with this constraint there would be no loss of reagents and this would minimize by-products in the process. In the

Table 1. The statistical experimental design 2^{8-4}_{IV} and responses.

Experiment #	Experimental variables[a]								Response[b]			
	x_1	x_2	x_3	x_4	x_5	x_6	x_7	x_8	y_1	y_2	y_3	y_r
1	−1	−1	−1	−1	−1	−1	−1	−1	25.3	73.5	0.80	0.40
2	+1	−1	−1	−1	+1	+1	+1	−1	14.3	73.9	6.48	5.32
3	−1	+1	−1	−1	+1	+1	−1	+1	6.0	91.6	1.36	1.04
4	+1	+1	−1	−1	−1	−1	+1	+1	19.6	78.8	0.95	0.65
5	−1	−1	+1	−1	+1	−1	+1	+1	6.9	90.7	1.21	1.19
6	+1	−1	+1	−1	−1	+1	−1	+1	11.8	87.0	0.72	0.48
7	−1	+1	+1	−1	−1	+1	+1	−1	12.3	85.6	1.37	0.73
8	+1	+1	+1	−1	+1	−1	−1	−1	8.9	88.6	1.24	1.26
9	−1	−1	−1	+1	−1	+1	+1	+1	0.5	97.5	1.68	0.32
10	+1	−1	−1	+1	+1	−1	−1	+1	0.0	96.0	3.46	0.54
11[c]	−1	+1	−1	+1	+1	−1	+1	−1	0.1	98.1	0.73	1.07
12	+1	+1	−1	+1	−1	+1	−1	−1	1.0	97.2	1.29	0.51
13	−1	−1	+1	+1	+1	+1	−1	−1	0.0	95.2	3.83	0.97
14	+1	−1	+1	+1	−1	−1	+1	−1	6.9	90.7	1.40	1.00
15	−1	+1	+1	+1	−1	−1	−1	+1	13.0	85.3	0.89	0.81
16	+1	+1	+1	+1	+1	+1	+1	+1	0.0	95.9	2.39	1.71

[a]Experimental variables: x_k (definition) [−1 level, +1 level]; x_1 (amount of K_2CO_3) [7 mmol, 14 mmol]; x_2 (catalyst NaI) [0, 1 mmol]; x_3 (concentration in DMF) [1:4 g ml^{-1}, 1:6 g ml^{-1}]; x_4 (1-chloroethyl ethyl carbonate) [10 mmol, 13 mmol]; x_5 (reaction temperature) [50°C, 70°C]; x_6 (reaction time) [8 h, 20 h]; x_7 (addition temperature) [20°C, 70°C]; x_8 (addition time) [0 min, 15 min]. [b]y_1 HPLC area% of **1**; y_2 HPLC area% of **3**; y_3 HPLC area% of by-product; $y_r = 100 - \sum_{i=1}^{3} y_i$.

[c]Experiment # 11 was replicated to obtain the percentage areas: [0.5, 98.0, 0.73].

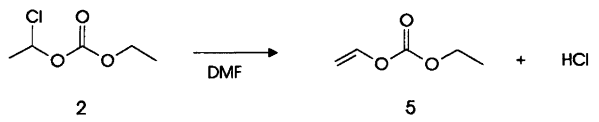

2 5

Scheme 3.

present case, however, the amount of the agent 1-chloroethyl ethyl carbonate should possibly be larger than the stoichiometric amount since there is a risk that the agent may be destroyed through an elimination reaction[9] of hydrogen chloride leading to the formation of vinyl ethyl carbonate **5**[10] as shown in Scheme 3.

Reaction temperature x_5. This variable is examined to monitor how the temperature influences the reaction rate, product yield, and possibly also how it influences the yield of side reactions.

Reaction time x_6. The reaction time is defined as the run time before quenching of the reaction mixture. This variable is believed to be important, both for the purity of the crude product, and for the economy of the process. Too long a reaction time will lead to unnecessary occupation of process equipment.

Addition temperature for **2** x_7. The variation of the addition temperature was chosen to be equal to or lower than the final reaction temperature. With a decreased mixing temperature at the addition point for the agent, the reaction might be expected to proceed in a more controlled way. Thus, side reactions may be depressed or eliminated.

Addition time of **2** x_8. The addition time was chosen to be as short as possible (low) or 15 min (high). Slow addition may prevent high local concentrations of the agent in the reaction mixture, which may (like variable x_4) give rise to undesired reactions such as the formation of vinyl ethyl carbonate **5** as shown in Scheme 3.

Table 1 gives an overview of the control variables x_1, x_2, ..., x_8 as well as the selected low (− 1) and high (+ 1) levels. To investigate each combination of two levels (full factorial design, 2^k) would yield a total of 256 experimental runs which, obviously, is too large a number of individual experiments. A full factorial design would make it possible to determine an average result, main effects of all variables as well as all interaction effects between the variables. For chemical reactions it is often found that interaction effects between three or more variables are negligible compared with main effects and two-variable interactions. For this reason, sufficiently good information as to the influence of the experimental variation on the observed results can be provided by estimates of the main effect and two-variable interaction effects.

Such information can be obtained by a fractional factorial design which selects a subset of all 256 possible combinations in such a way that main effects and two-variable interaction effects can be independently estimated. For details of the construction of factorial and fractional factorial designs, see Box *et al.*[11–13] In the present case a 2^{8-4} fractional factorial design (with 16 runs) was used, Table 1. This design is a resolution IV design[14] by which all main effects can be estimated without confounding[15] with two-variable interaction effects. However, two-variable interactions will be confounded by each other, see Table 2. Nevertheless, from the confounded interaction effects it is possible to discern whether there are significant interactions among the variables.

A model which relates the observed response, y, to the experimental variables x_k, $k = 1$–8 and which accounts for these features is a linear model to which confounded cross-product terms have been added.

$$y_i = \beta_0 + \sum_{k=1}^{K} \beta_k x_k + \sum_{k>l}^{K} \beta_{kl} x_k x_l + \varepsilon_i \qquad (1)$$

Table 2. The numerical estimates for the main effects and the two-factor interactions.

Variables and confounding pattern for the two-factor interactions		Estimate
β_0	Mean yield of **3**	89.100
β_1	Amount of potassium carbonate	−0.588
β_2	Amount of sodium iodide	+1.038
$\beta_{12}+\beta_{35}+\beta_{46}+\beta_{78}$		+0.575
β_3	Concentration of substrate in DMF	+0.775
$\beta_{13}+\beta_{25}+\beta_{68}+\beta_{47}$		+1.263
$\beta_{23}+\beta_{15}+\beta_{67}+\beta_{48}$		−2.063
β_5	Reaction temperature	+2.150
β_4	Amount of 1-chloroethyl ethyl carbonate	+5.387
$\beta_{14}+\beta_{26}+\beta_{37}+\beta_{58}$		+1.050
$\beta_{24}+\beta_{16}+\beta_{57}+\beta_{38}$		−1.400
β_6	Reaction time	+1.388
$\beta_{34}+\beta_{17}+\beta_{56}+\beta_{28}$		−3.487
β_7	Addition temperature	−0.200
β_8	Addition time	+1.250
$\beta_{18}+\beta_{27}+\beta_{36}+\beta_{45}$		−0.338

The regression coefficients, β_k and β_{kl}, were estimated by least-squares fitting of the screening model to the observed results. The regression coefficients which have significant influence in the model were determined by using a cumulative normal probability plot,[16] shown in Fig. 1. An overview of the estimated regression coefficients with confounding patterns for the two-factor interaction terms is given in Table 2.

Four of the variables were found to have significant influence on the yield of the synthesis. Two variables, x_4, x_5 have significant main effects and the two others, x_1, x_6 have influence through interaction effects (antagonistic) in combination with the variables which also showed significant main effects.

The regression coefficients which are outside the range of the experimental error variation, are main effects, $\beta_4 = +5.387$ and $\beta_5 = +2.150$, aliased interaction effects, $\beta_{23}+\beta_{15}+\beta_{67}+\beta_{48} = -3.487$, $\beta_{24}+\beta_{16}+\beta_{57}+\beta_{38} = -1.400$, and $\beta_{34}+\beta_{17}+\beta_{56}+\beta_{28} = -3.487$, see Fig. 1. For the confounded interaction effects, the most probable antagonistic effects are β_{15}, β_{16} and β_{56}. This conclusion was also supported by subsequent test runs. The mathematical expression obtained for the yield of **3** is given in eqn. (2).

$$y = \beta_0 + \beta_4 x_4 + \beta_5 x_5 + \beta_{15} x_1 x_5 + \beta_{16} x_1 x_6 + \beta_{56} x_5 x_6 \quad (2)$$

The final model [eqn. (2)], was then used to predict the results for the experiments carried out. The accordance between the predicted value with the experimental value is acceptable. The statistics, the root mean square of error prediction parameters, RMSEP = 2.95 and the multiple correlation coefficient, $R^2 = 0.86$ also indicate the good predictive capability of the model. The cumulative normal probability plot of the residuals in Fig. 2 shows, however, that the experiments 3 and 16 show slight deviations in predicted values compared with the experimental results.

The modelling shows that the variables which have significant influence on the response yield of **3** are x_1, x_4, x_5 and x_6, and the deviation for experiments 3 and 16 are likely to be due to errors in measuring the response or to unusually large errors in the experimental execution.

These two experiments also explain the aberrant observation in the normal probability plot of the estimated regression coefficients: the two parallel straight lines which 'break apart' close to the zero value on the abscissa, and thus divide positive effect values from the negative effect values. For a discussion of such phenomena, see Ref. 17.

Fig. 3 shows the isocontour projections of the response surfaces for the yield of **3**. In these projections, the two most influential variables, x_4 and x_5, are varied continuously, while the other significant variables, x_1 and x_6, are set to all combinations of low and high levels, respectively. Thus, Fig. 3 portrays a five-dimensional response surface.

Optimal reaction time. In order to determine an optimal reaction time, fiber-optical near infrared spectroscopy[18] (NIR) was used to monitor the reaction *in situ*. The PCA

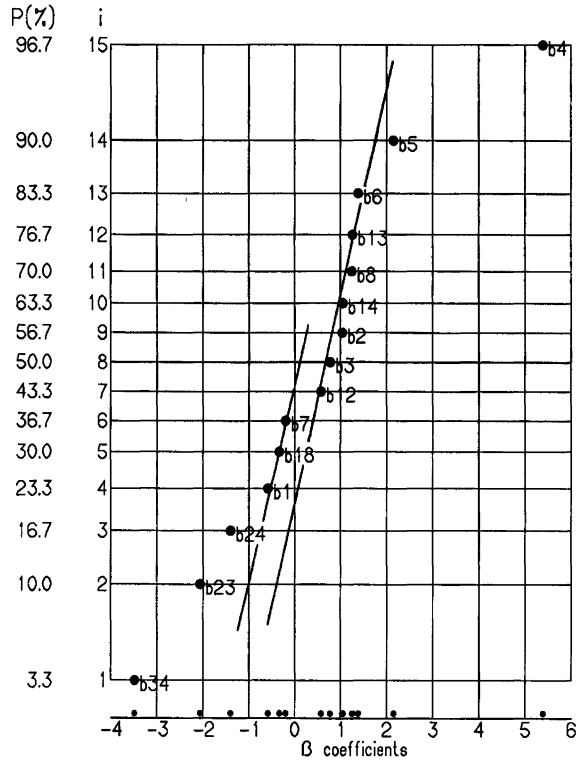

Fig. 1. Cumulative normal probability plot of the regression coefficients.

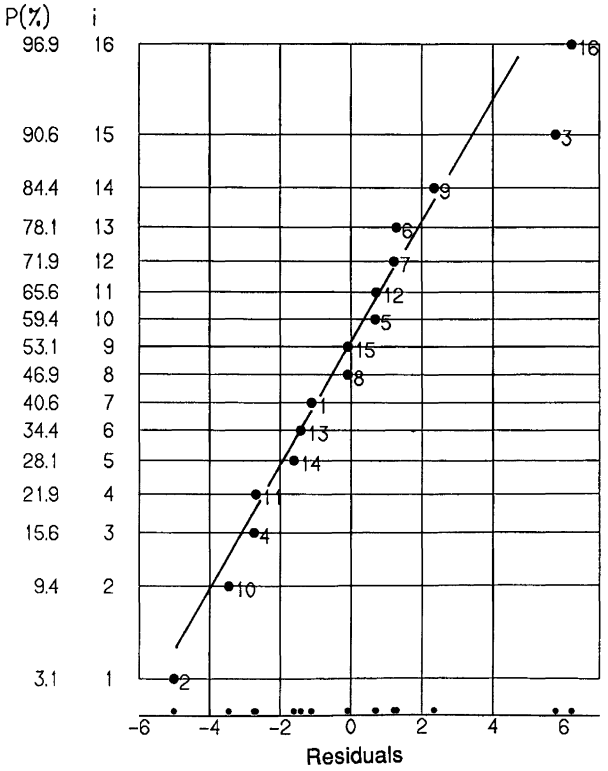

Fig. 2. Cumulative normal probability plot of the residuals.

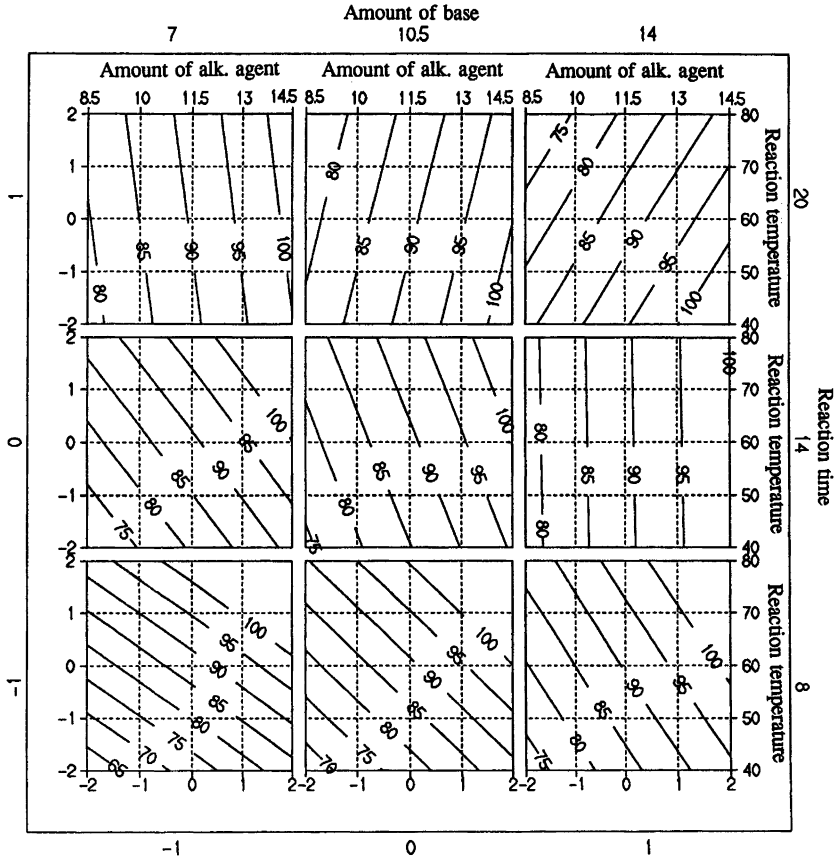

Fig. 3. Contour plots of the response surfaces showing the yield of **3**. The plots show the variations of the responses when four experimental variables are varied. To read the plot, the large frame shows the variation in reaction time (x_6) and amount of potassium carbonate (x_1). In this frame, nine subplots showing the contour projections of the surface when the amount of 1-chloroethyl ethyl carbonate (x_4) and the reaction temperature (x_5) are varied. For instance, the variation in response for the settings $x_1 = -1$, $x_6 = -1$ and the varying of x_4 and x_5 is shown in the subplot in the lower left-hand corner of the figure. Other settings are evaluated analogously. The plot actually describes variation in five dimensions.

(principal components analysis[19]) method was applied to simplify and interpret the sampled complex NIR spectra. The spectra, which contain 1201 data points, were ordered in sequences (63 samplings times) to yield a 63×1201 X matrix.

The PCA method corresponds to factorization of the data matrix X (which in this case are $i = 1, 2, \ldots, I$ NIR spectra, each with $k = 1, 2, \ldots, K$ wavelength) into means ($\bar{x}_k$), scores (t_{ia}), loadings (p_{ak}) and residuals (ε_{ik}), and can be described mathematically by eqn. (3).

$$x_{ik} = \bar{x}_k + \sum_{a=1}^{A} t_{ia} p_{ak} + \varepsilon_{ik} \qquad (3)$$

The first principal component describes the largest systematic variation in the data matrix X, the second describes the next largest and so on. The number of principal components, A, is much smaller than the number of variables, K. Hence, the PC model gives a considerable simplification. In order to determine the optimal number of principal components ($a = 1, 2, \ldots, A$), the cross validation method[20] was used, with 63 cross-validation elements randomly selected. A two principal component model ($A = 2$) was determined, where the variance for principal component #1 was 99.2% and for principal component #2 0.8%.

The scores t_{ia} show the location of the spectral information for spectrum i (object) along the ath principal component and hence, describe the between-object variation. Spectra which are similar will thus have similar score value. When the composition of the reaction mixture changes between the sampling times, the corresponding score values will be different. As the reaction approaches its final state, the score values will asymptotically approach a constant value.

The loadings p_{ak} describe the within-object variation of the spectral signals. The absolute value of the loadings, p_{ak}, tells how much a certain wavelength contributes to the ath principal component, and the signs give the information as to whether a particular wavelength is negatively or positively correlated with the principal component.

A plot of estimated scores (t_a) versus reaction time is shown in Fig. 4. Since the score values are linear combinations of the absorbances and hence related to con-

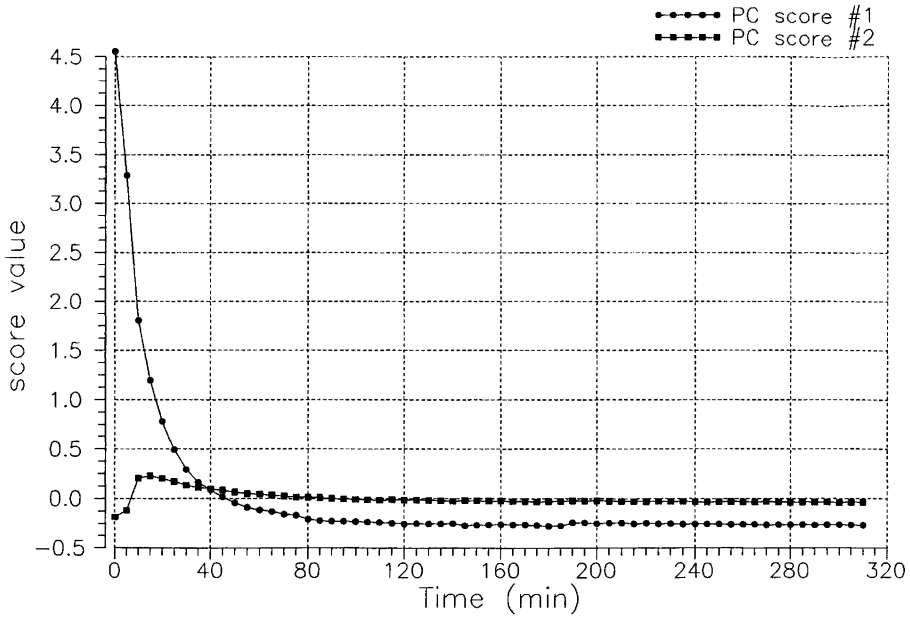

Fig. 4. Plot of results from principal components analysis on NIR spectra. Time in minutes on the abscissa versus estimated score values on the ordinate.

centration of the constituents of the reaction mixture, a score versus time plot may be considered as a concentration profile over time.

The optimal reaction time (x_6) was determined from the plot as the time at which the scores have reached their final constant value. This optimum reaction time was determined to be $t = 90$ min (x_6).

Computing. In-house developed software *SynDe* (*Synthesis Design*) written in Zortech C/C++ V3.0 was used to create the experimental design, to plot the cumulative normal probability graphs, and to simulate and plot the response surfaces. Other graphs were created by using Grapher™.[21] Unscrambler II version 5.00 software was used to estimate the regression coefficients using the partial least-squares regression (PLSR) method,[22] and to estimate the principal component scores using the principal components analysis method. All the computation was performed under DOS 5.0 on a COMPAQ DESKPRO 50M and 32 bit i486 microprocessor-based microcomputer.

Discussion and conclusion

The amount of potassium carbonate (x_1) has an influence on the synthesis due to interaction effects with temperature (increasing the base activity) and with reaction time (x_6). Both cross products show antagonistic behaviour of the variables on the yield of **3**. These results were expected. An increase in reaction temperature and high base concentration promote the degradation of the base-labile reagent **2** which results in a lowered yield of **3**. Long reaction time at high base concentration leads to hydrolytic degradation of **3**.

The formation of a carbonate ester in the synthesis of pivampicillin has been reported to be catalyzed by iodide ions.[8] This reaction is very similar to the reaction discussed in the present paper. It was therefore surprising that the presence or absence of iodide ions (variable x_2) did not influence the final yield. This shows that iodide is not a general catalyst for this type of reaction.

The variation of concentration of the substrate (x_3), does not show any significant effect on the reaction, either as a single variable or in interaction with other variables. From a practical point of view, this was a highly satisfactory result, since this makes it possible to achieve a high capacity in preparative runs.

The amount of **2** (x_4), and the temperature (x_5) both have positive coefficients, which implies that an excess of the agent and 'high' temperature should be used for obtaining a high yield of the product **3**. However, the temperature shows negative interactions with the variable x_1, as well as with variable x_6. This implies that an optimal temperature setting is dependent on the setting of variables x_1 and x_2. The variation in the settings of x_7 (addition temperature) and x_8 (addition time), respectively, do not have any influence on the yield.

At the outset of the present study, eight experimental variables were considered as potentially important. An experimental design with 16 runs made it possible unequivocally to identify four variables as important. These results show the merits of statistically designed experiments.

The conclusion as to the influence of the experimental variables was fully confirmed in pilot-plant scale synthesis.

Principal components analysis of NIR spectra recorded during the course of the reaction is a new tech-

nique which may hopefully be developed into a general method for reaction monitoring since NIR spectra can be recorded at short intervals. Such a technique would be more convenient than chromatographic analysis.

Experimental

Chemicals. The acid **1** was obtained from Nycomed. The reagent, chemicals and solvents were obtained from Fluka and Jansen Chimica.

General procedure for the screening experiment. Settings of the variables in the individual runs and the results obtained are summarized in Table 1. The acid **1** (10 mmol), the given amount x_1 of potassium carbonate, and the given amount x_2 of sodium iodide as catalyst were dissolved in the given amount x_3 of DMF. The given amount x_4 of 1-chloroethyl ethyl carbonate **2** was added to the solution. The addition was carried out over the given addition time x_8, at the given addition temperature x_7. When the addition was complete, the temperature of the reaction mixture was adjusted to x_4. Samples were withdrawn at the reaction time x_6 and analyzed by HPLC, see below.

Optimized synthetic procedure. The acid **1** (10 mmol) was mixed with potassium carbonate (7 mmol) in DMF in concentration 1:5 w/v. 1-Chloroethyl ethyl carbonate (13.0 mmol) was then added in one portion. The reaction was performed at a temperature of 75°C with a reaction time of 90 min.

Chemical analysis. The reaction mixture was analyzed by reversed-phase HPLC to determine the amounts of product, by-product, and unchanged substrate. Integrated peak areas were used for quantification.

HPLC set-up and eluents. Two eluents, A and B, were used where eluent A was prepared by dissolving 1500 µl phosphoric acid in 1000 ml purified water, and eluent B was prepared by dissolving 1500 µl phosphoric acid in a mixture of 500 ml purified water and 500 ml acetonitrile. The eluents were degassed with helium prior to use.

The solvent-delivery system consisted of gradient pumping 20–100% of eluent B, for 50 min, isocratic pumping 100% of eluent B for 10 min and finally equilibration 20% of eluent B for 12 min with a flow rate of 1.0 ml min^{-1}. The column used was RP-18, Brownlee Columns (L 250 mm, ID 4.6 mm) and particle size 5 µm. A UV detector operating at wavelength $\lambda = 254$ nm was used.

Sample preparation. The reaction mixture was quenched by addition of 1.4 equiv. (0.8 ml, 14 mmol) acetic acid which efficiently stopped the reaction. The mixture was then diluted with solution B to yield a 0.15% solution in acetonitrile and water. An injected amount of 10 µl was used in the HPLC analysis.

Reaction monitoring by fiber-optical NIR spectroscopy. A fiber-optical NIR instrument Quantum 1200 Plus from LT-Industries with PbS detector for the wavelength region $\lambda = 1200–2400$ nm was used. The measurements were performed directly in the synthesis reactor by using a 1.5 m fiber-optical cable (125 in/125 out) connected to a 20 cm transreflectance steel probe with a sapphire window which was immersed in the reaction mixture. The instrument was controlled by a WYSE DECISION 486/25, an 486 25 Mz 32 bits microprocessor based microcomputer under DOS 5.0. The software SpectraMetrix, V1.70[23] supplied from LT-Industries was used to control the instrument.

An average of 30 scans (1200–2400 nm, scan speed 5 s^{-1}) was sampled each 5 min. The data were ordered in a data matrix in such a way that the first recorded NIR spectrum was the first row of the matrix, the second recorded was the second row, and so on. Thus the position of each spectrum also represented a time position. The matrix was subjected to multivariate data analysis by the PCA method using Unscrambler II software.

Acknowledgements. The author would like to express his gratitude to Department of Chemical Analysis at Nycomed Imaging AS for excellent technical assistance concerning the chemical analysis by HPLC. Nycomed Imaging AS is acknowledged for the permission to publish the present work. Dr. Rolf Carlson is acknowledged for valuable hints and discussions throughout the present work. Special gratitude is due to computer programmer Mikael Ørseng who has converted my requirements concerning the experimental design and graphics to functional codes in the software *SynDe*.

References

1. Jansen, A. B. A. and Russell, T. J. *J. Chem. Soc.* (1965) 2127.
2. Sovak, M. In: Sovak, M., Ed., *Radiocontrast Agents*, Springer-Verlag, Berlin 1984, introduction; Hoey, G. B. and Smith, K. R. In: Sovak, M., Ed., *Radiocontrast Agents*, Springer-Verlag, Berlin 1984, Chap. 1.
3. Udupa, J. K. In: Udupa, J. K. and Herman, G. T., Eds., *3D Imaging in Medicine*, CRC Press, Boca Raton, Florida 1991, Chap. 1.
4. Vannier, M. W., Hildebolt, C. F., Gayou, D. E. and Marsh, J. L. In: Udupa, J. K. and Herman, G. T., Eds., *3D Imaging in Medicine*, CRC Press, Boca Raton, Florida 1991, Chap. 2.
5. Gjøen, T., Holtz, E., Strande, P., Klaveness, J., Leander, P. and Berg, A. In: Ferrucci, J. T. and Stark, D. D., Eds., *Liver Imaging, Current Trends and New Techniques*, Andover, Boston 1990, Chap. 45.
6. Miller, J. A. and Nunn, M. J. *J. Chem. Soc., Perkin Trans. 1* (1976) 416.
7. Roberts, J. D. and Caserio, M. C. *Basic Principles of Organic Chemistry*, 2nd Ed., Benjamin, Menlo Park, CA 1977, pp. 230–233.
8. *Comprehensive Medicinal Chemistry, The Rational Design, Mechanistic Study and Therapeutic Application of Chemical Compounds*, Vol. 2, *Enzymes and Other Molecular Targets*, Sammes, P. G., Ed., Pergamon Press, Oxford 1990, p. 622.

9. Baciocchi, E. In: Patai, S. and Rappoport, Z., Eds., *The Chemistry of Functional Groups, Suppl. D*, Part 2, pp. 1173–1227, Wiley, New York 1983.
10. Archarya, S. P. and Brown, H. C. *J. Chem. Soc., Chem. Commun.* (1968) 305.
11. Box, G. E. P. and Hunter, J. S. *Technometrics 3* (1961) 311.
12. Box, G. E. P. and Hunter, J. S. *Technometrics 3* (1961) 449.
13. Box, G. E. P., Hunter, W. G. and Hunter, J. S. *Statistics for Experimenters, an Introduction to Design, Data Analysis and Model Building*, Wiley, New York 1978, pp. 306–351, 374–418.
14. Box, G. E. P., Hunter, W. G. and Hunter, J. S. *Statistics for Experimenters, an Introduction to Design, Data Analysis and Model Building*, Wiley, New York 1978, pp. 398–404.
15. Box, G. E. P., Hunter, W. G. and Hunter, J. S. *Statistics for Experimenters, an Introduction to Design, Data Analysis and Model Building*, Wiley, New York 1978, pp. 381–390, 411–412.
16. Daniel, C. *Technometrics 1* (1959) 311.
17. Box, G. E. P. and Draper, N. R. *Empirical Model-Building and Response Surfaces*, Wiley, New York 1987, pp. 131–134.
18. Osborne, B. G. and Fearn, T. *Near Infrared Spectroscopy in Food Analysis*, Longman, Essex 1986, pp. 1–85.
19. Jolliffe, I. T. *Principal Component Analysis*, Springer-Verlag, New York 1986, pp. 1–114.
20. Wold, S. *Technometrics 20* (1978) 397.
21. Grapher™ Reference Manual, Version 3.0, Golden Software Inc., Golden, Colorado, USA.
22. Unscrambler II, Extended Memory Version 5.00. User's Guide, June 1993. CAMO A/S, Olav Tryggvasonsgt. 23, N-7011 Trondheim, Norway.
23. SpectraMetrix, V1.70 Reference Manual, January 1989. L.T. Industries, Inc., 6110 Executive Boulevard, Rockville, MD 20852, USA.

Received November 8, 1993.